

Magnetic dipole radiation tailored by substrates: numerical investigation

Dmitry L. Markovich^{1*}, Pavel Ginzburg^{2**}, Anton Samusev¹,
Pavel A. Belov¹, and Anatoly V. Zayats²

¹ St. Petersburg National Research University of Information Technologies, Mechanics and Optics, 49 Kronverskii Ave., St. Petersburg 197101, Russian Federation

² Department of Physics, King's College London, Strand, London WC2R 2LS, UK

Corresponding author: *dmmrkovich@gmail.com, **pavel.ginzburg@kcl.ac.uk

Nanoparticles of high refractive index materials can possess strong magnetic polarizabilities and give rise to artificial magnetism in the optical spectral range. While the response of individual dielectric or metal spherical particles can be described analytically via multipole decomposition in the Mie series, the influence of substrates, in many cases present in experimental observations, requires different approaches. Here, the comprehensive numerical studies of the influence of a substrate on the spectral response of high-index dielectric nanoparticles were performed. In particular, glass, perfect electric conductor, gold, and hyperbolic metamaterial substrates were investigated. Optical properties of nanoparticles were characterized via scattering cross-section spectra, electric field profiles, and induced electric and magnetic moments. The presence of substrates was shown to introduce significant impact on particle's magnetic resonances and resonant scattering cross-sections. Variation of substrate material provides an additional degree of freedom in tailoring properties of emission of magnetic multipoles, important in many applications.

1 Introduction

Materials can respond to applied electromagnetic field via both electric and magnetic susceptibilities. While dielectrics demonstrate relatively high values of permittivities even at high frequencies (ultraviolet spectral range or lower), inherent natural permeabilities rapidly approach unity, having certain high-frequency cut-off around MHz frequencies [1]. This natural property results from relatively fast electronic polarizabilities and electronic band structure that has resonances at optical frequencies and slow spin and orbital interactions which define the magnetic susceptibility. Nevertheless, optical magnetism can be artificially created via carefully engineered subwavelength structures. For example, arrays of ordered split-ring resonators, made of conducting metals, can create artificial magnetic responses at high frequencies (THz range) and even produce negative effective permeabilities [2]. Similar concepts can be also employed in optics. With proper choice of shape of metallic nanostructures and their arrangements, called metamaterials, artificial magnetism has been demonstrated in the infra-red and visible spectral range [3, 4, 5, 6]. One of the fundamental bottlenecks, limiting the performance of plasmonic components and metamaterials is inherent material losses that is of great importance for various nanophotonic components, such as nanolenses [7, 8], antennas [9], particle-based waveguides [10], ordered particle arrays [11], and biosensors [13]. At the same time, high refractive index dielectric nanoparticles have shown to be promising in the context of artificial magnetism and the majority of aforementioned components can be implemented with all-dielectric elements, as was already demonstrated in case of ordered particle arrays [12] and antenna applications [14]. Resonant phenomena in positive permittivity particles, in contrary to subwavelength plasmonic structures, rely on the retardation effects. Nevertheless, high index spherical particles of nanometric dimensions can exhibit multiple resonances in the visible spectral range. In particular, strong resonant light scattering associated with the excitation of magnetic and electric dipolar modes in silicon nanoparticles has recently been demonstrated experimentally using dark-field optical microscopy [15, 16] and directional light scattering by spherical silicon nanoparticles in the visible spectral range has been reported [17]. While the majority of theoretical studies consider isolated spherical particles or their clusters in free space, very often experimental geometries involve the presence of substrates where nanoparticles are placed [15, 16, 17]. Therefore, investigations of substrate effects on magnetic dipole resonances in dielectric nanoparticles are of great importance for understanding both fundamental phenomena and predictions of experimental measurements. In this paper, we performed numerical studies of optical properties of high-index dielectric nanoparticles on various types of substrates. In particular, glass, gold and hyperbolic metamaterial substrates were considered. Optical

properties of nanoparticles were characterized via scattering cross-section spectra, electric field profiles, and induced electric and magnetic moments.

2 Theoretical and numerical frameworks

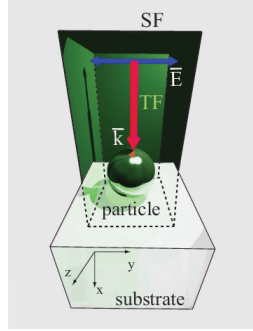


Fig. 1: Dielectric nanoparticle on a substrate illuminated with a plane wave. The regions inside and outside the green box depicts total (incident and scattered) electric field (TF) and scattered electric field (SF), respectively.

Optical response of individual spherical particles embedded in homogeneous host materials can be described analytically via the Mie series decomposition [18]. Generally, any shape with boundaries belonging to “coordinate surfaces” sets at coordinate systems where Helmholtz equation is separable, i.e., has analytic solution for scattering problems. However, the separation of variables method breaks down once substrates are introduced. As the first order approximation, the image theory could be employed [19, 20, 21], while more complex treatments can account for retardation effects and higher multi-pole interactions [22, 23, 24]. Considerations of anisotropic substrates lead to major complexity even in the image theory (point charge images should be replaced by certain distributions) [25] and make fully analytical approaches to be of limited applicability. Moreover, in the case of high-index dielectric particles, the resonances are overlapping in frequency, making even the image theory to be inapplicable. At the same time, this spectral overlap can be employed for super-directive antenna applications [16, 26].

One of the commonly used techniques for numerical analysis of scattering processes is the so-called “total-field scattered-field”(TFSF) approach [27]. The key advantage of this method is the separation of relatively weak scattered field (SF) from predominating high amplitude total field (TF) which contains both incident and scattered fields, in a distinct simulation domain. The TFSF method also allows to subtract the electric field, reflected backwards by the substrate in the SF domain, enabling the calculation of a scattering cross-section.

The geometrical arrangement of the considered scenario is represented in Fig. 1: a small dielectric spherical particle ($r = 70$ nm, $\epsilon = 20$) is placed on the substrate. The centre of the particle coincides with the coordinate origin. The system is illuminated with a short pulse (in time) with broadband spectrum covering the spectral range from 400 to 750 nm. FDTD method allows analyzing spectral responses via single simulation by adopting the Fourier decomposition method with subsequent normalization. The key parameters characterizing the system are the electric and magnetic dipole moments defined as

$$\begin{aligned} \mathbf{p} &= \epsilon_0 \iiint_{V_{sphere}} (\epsilon(r, \omega) - 1) \mathbf{E}(r, \omega) dV \\ \mathbf{m} &= \frac{i\omega \cdot \epsilon_0}{2} \iiint_{V_{sphere}} (\epsilon(r, \omega) - 1) \mathbf{E}(r, \omega) \times \mathbf{r} dV, \end{aligned} \quad (1)$$

where ϵ_0 is the vacuum permittivity, $V_{sphere} \simeq 1.44 \times 10^{-3} \mu\text{m}^3$ is the volume of the particle, $\epsilon(r, \omega)$ is the frequency-dependent particle permittivity, ω , is the frequency of the incident light, and $\mathbf{E}(r, \omega)$ is the electric field in frequency domain. Generally, these dipolar moments in the asymmetric system considered here depend on the illumination polarization, direction of incidence and spatial shape of the beam. In the following, a normally incident y-polarized plane wave was considered. To avoid the interplay between geometrical parameters and chromatic dispersion of the particle’s material, the latter was neglected.

3 Results and discussion

3.1 Optical properties of a dielectric nanoparticle in free space

To verify the accuracy of the approach, optical properties of the particle in free space were evaluated numerically and compared to analytic description. Scattering cross-section spectra (Fig. 2(a)) shows 3 distinctive resonances corresponding to magnetic dipole (MD), electric dipole (ED), and magnetic quadrupole (MQ) at 644 nm, 472 nm, and 444 nm, respectively. The corresponding electric field amplitude distributions are depicted on Fig. 2(c, d, and e). They show the amplification of near field amplitude with respect to the input source field and provide visual hints for identification of the type of a resonance. The circular-like electric field distribution is observed for a MD resonance (Fig. 2e), the drop-shaped distribution for an ED resonance (Fig. 2d), and the double resonant sectors for a MQ resonance (Fig. 2c).

Knowing the electric field distribution in the entire space allows to calculate the moments defined in Eq. 1. These results are summarized in Fig. 2(b). Since the particle is illuminated along the x-axis with the y-polarized plane wave, the electric moment component p_y and magnetic moment component m_z are expected to be dominating. Having calculated all other components for both electric and magnetic moments, we found p_y and m_z to be more than $1e^{17}$ times larger than other components, confirming symmetry arguments. It is instructive to compare the obtained values to the induced electric dipolar moment of a gold sphere of the same radius [28] which is $p_{gold} = 2.58e^{-4}$ [e·nm] at 472 nm; hence, a high-index dielectric particle has ≈ 4 times larger electric dipolar moment and no associated material losses. Numerically calculated dipolar moments were compared with analytical Mie theory approach reported in [12] and differ by no more than 5%, verifying the accuracy of the employed numerical method.

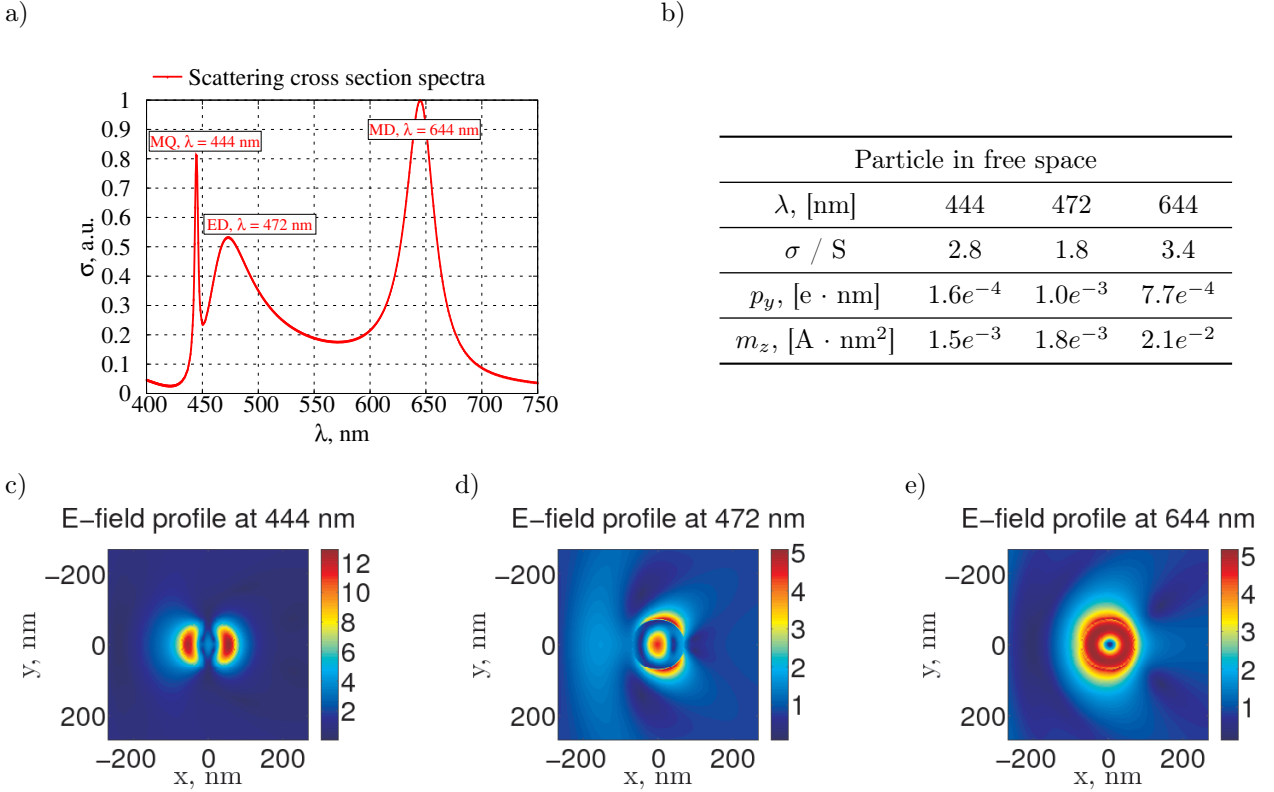
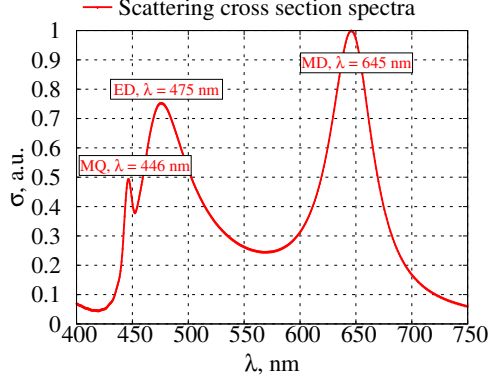


Fig. 2: Optical properties of a dielectric ($\epsilon_{particle} = 20$) nanoparticle of 70 nm radius in free space: (a) scattering cross-section spectra, (b) the summary of the resonant wavelengths, the scattering cross-section normalised to the geometric cross-section, and electric p_y and magnetic moments m_z , (c-e) the spatial distribution of the electric field amplitudes at resonant wavelengths (normalised to the incident field).

3.2 Dielectric substrate

In many cases, dielectric particles are placed on glass substrates as the result of their fabrication and for optical characterisation [17]. This type of substrates is expected to introduce the smallest distortions in the optical properties of a particle, compared to other types of substrates, e.g., metallic ones. We considered a glass substrate with $\epsilon = 3.1$ corresponding to the family of flint glasses. Comparing to the nanoparticles in free space, the glass substrate influence is in significant suppression of the high-order multipoles (Fig. 3), with both electric and, especially, magnetic dipolar resonances being less affected. These conclusions are confirmed by the field amplitude distributions at the resonant wavelengths. Minor electric field amplitude amplification for ED and MD resonance and nearly two times reduction for MQ resonance can be seen compared to the particle in free-space. The electric moment of the particle is slightly increased while the magnetic one is slightly reduced.

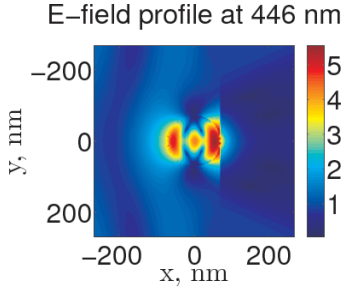
a)



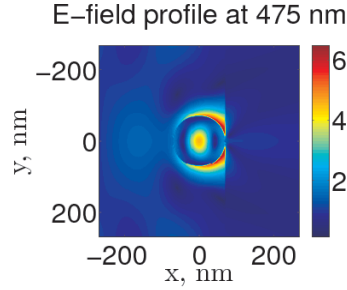
b)

Particle on a dielectric substrate			
λ , nm	446	475	645
σ / S	1.5	2.3	3.0
p_y , [e · nm]	$2.44e^{-4}$	$1.1e^{-3}$	$9.8e^{-4}$
m_z , [A · nm ²]	$1.3e^{-3}$	$1.2e^{-3}$	$1.5e^{-2}$

c)



d)



e)

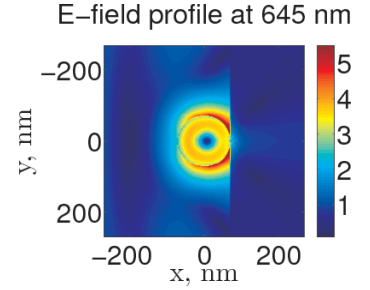


Fig. 3: Optical properties of a dielectric nanoparticle ($\epsilon_{particle} = 20$) of 70 nm radius on a dielectric substrate ($\epsilon_{dielectric} = 3.1$): (a) scattering cross-section spectra, (b) the summary of the resonant wavelengths, the scattering cross-section normalised to the geometric cross-section, and electric p_y and magnetic moments m_z , (c-e) the spatial distribution of the electric field amplitudes at resonant wavelengths (normalised to the incident field).

3.3 PEC substrate

In order to test the applicability of the image theory for high-index dielectric particles, a perfect electric conductor (PEC) substrate was considered. This dispersionless metal with infinitely large imaginary part of the permittivity acts like a perfect mirror for both electromagnetic waves and point charges. The results for a PEC substrate are summarized in Fig. 4. Compared the free space, a PEC substrate leads to the spectral shift of the nanoparticle resonances and significant modifications of the spectrum and magnitude of the scattering cross-sections. For example, the electric dipole, induced in the direction parallel to the surface, should create the contra-oriented image dipole and, as the result, the resulting dark quadrupolar resonance of the system should suppress the scattering (as in the case of subwavelength plasmonic particles). Nevertheless, the electric dipole resonance became the strongest in the presence of PEC. This effect is related to the retardation, since the optical path between the dielectric sphere and its image become comparable to wavelength due to the high-index dielectric. Near-field amplitudes are almost three-fold increased compared to free space as the result of perfect reflection of the incident wave by the substrate. Both electric and magnetic moments in this case experience strong resonant amplification by almost two orders of magnitude.

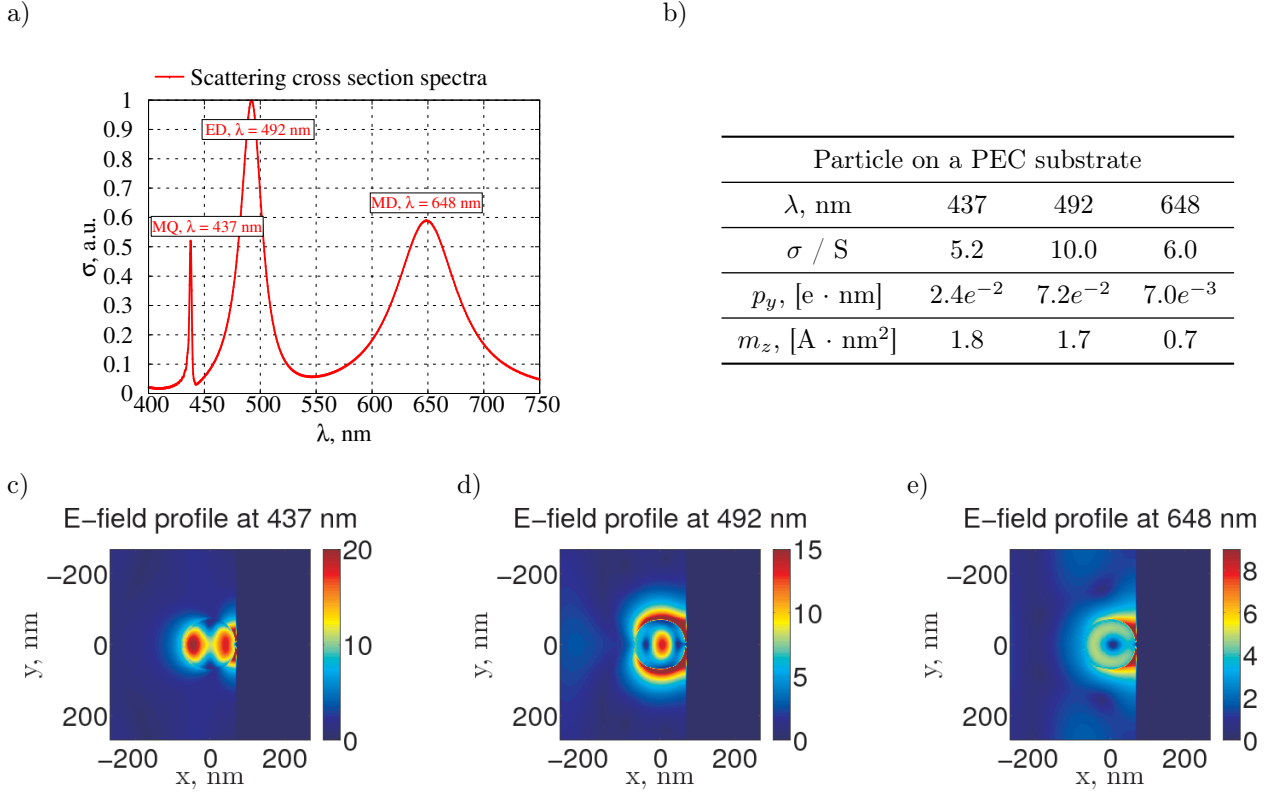
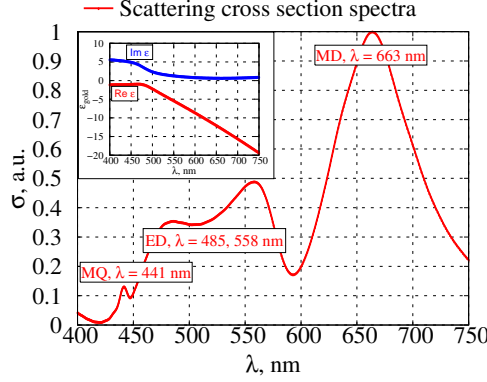


Fig. 4: Optical properties of a dielectric nanoparticle ($\epsilon_{particle} = 20$) of 70 nm radius on a PEC substrate ($\epsilon_{PEC} = 1 + 1e^6i$): (a) scattering cross-section spectra, (b) the summary of the resonant wavelengths, the scattering cross-section normalised to the geometric cross-section, and electric p_y and magnetic moments m_z , (c-e) the spatial distribution of the electric field amplitudes at resonant wavelengths (normalised to the incident field).

3.4 Gold substrate

The illumination of a scatterer placed on a gold film gives rise to excitation of surface plasmon polaritons [28]. The excitation of additional propagating surface wave substantially changes the optical properties of dielectric spheres (Fig. 5). It can be seen that the electric dipole resonance is split in two. This is the result of strong coupling by anti-crossing between two coupled dipoles (SPP mode and ED resonance of the particle). Moreover, the electric dipole mode excites the SPP with much higher efficiency than the other particle resonances. Electric field amplitudes experience minor amplification comparing to the case of free space, except for the MQ resonance. The electric moment experiences nearly ten fold enhancement due to the presence of the substrate, whilst the magnetic moments retain the values close to those in free space.

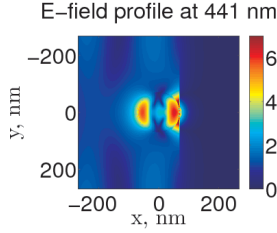
a)



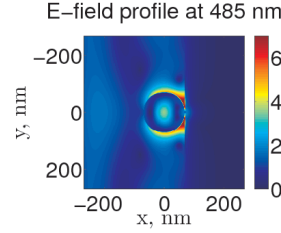
b)

Particle on a Au substrate				
λ, nm	441	485	558	663
σ / S	0.5	1.4	1.9	3.9
$p_y, [\text{e} \cdot \text{nm}]$	$7.0e^{-5}$	$1.1e^{-3}$	$2.3e^{-2}$	$1.7e^{-3}$
$m_z, [\text{A} \cdot \text{nm}^2]$	$1.6e^{-3}$	$1.5e^{-3}$	$5.2e^{-3}$	$1.2e^{-2}$

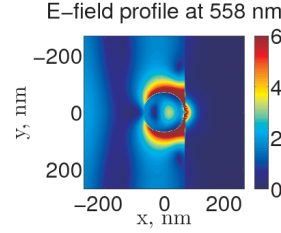
c)



d)



e)



f)

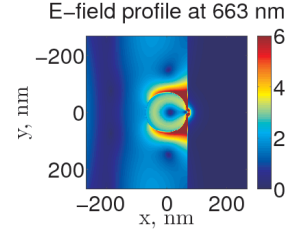


Fig. 5: Optical properties of a dielectric nanoparticle ($\epsilon_{\text{particle}} = 20$) of 70 nm radius on a gold substrate (inset if (a) shows ϵ_{gold} taken from [29]): (a) scattering cross-section spectra, (b) the summary of the resonant wavelengths, the scattering cross-section normalised to the geometric cross-section, and electric p_y and magnetic moments m_z , (c-e) the spatial distribution of the electric field amplitudes at resonant wavelengths (normalised to the incident field).

3.5 Metal-dielectric multilayered substrate: comparison between effective medium and composite representations

Hyperbolic metamaterials are artificially created media with strongly anisotropic effective permittivity tensors. They attract considerable attention due to their potential to substantially increase the local density of states and, as the result, increase radiative rate of emitters situated in their vicinity. Here, we consider the impact of a hyperbolic material substrates on the optical properties of high-index dielectric particles. One of the yet open questions is the applicability of effective medium theory to various physical scenarios considering an emitter (or scatterer) placed in the near-field proximity to a metamaterial [30, 31]. Hereafter, we compare the layered realization of hyperbolic metamaterial [32] with its homogeneous counterpart described via effective medium theory [33] neglecting the effects of spatial dispersion [34].

The considered nanostructured substrate consists of dielectric layers with $\epsilon_d = 3.1$ and silver metal layers with ϵ_m (the Drude model for silver for considered [29]). The layers have the same subwavelength thickness (30 nm) and can be described using a diagonalised effective permittivity tensor with components

$$\begin{aligned}\epsilon_{xx} &= \frac{\epsilon_d \cdot \epsilon_m}{(1 - \rho) \cdot \epsilon_d + \rho \cdot \epsilon_m} \\ \epsilon_{yy} = \epsilon_{zz} &= \rho \cdot \epsilon_d + (1 - \rho) \cdot \epsilon_m,\end{aligned}\quad (2)$$

where $\rho=0.5$ is the filling factor in the case of equal metal and dielectric layer thicknesses. These effective permittivity components are shown in Fig. 6.

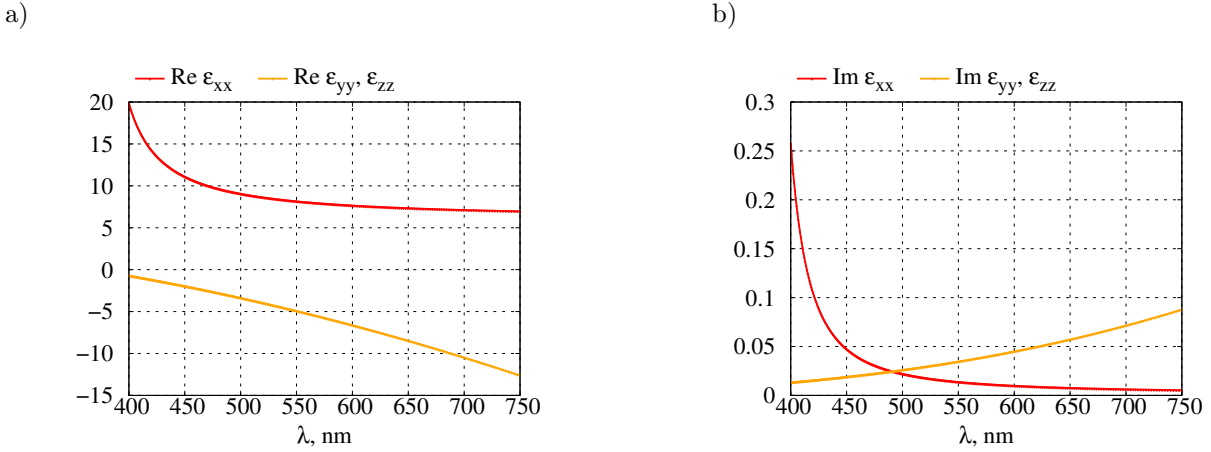


Fig. 6: Dispersion of the components of the effective permittivity $\epsilon_{xx}, \epsilon_{yy} = \epsilon_{zz}$, for the metamaterial substrate made of a silver-glass multilayer: (a) real and (b) imaginary parts.

The scattering cross-sections for the particle placed on the substrates made of the multilayered composite and the effective medium look very much alike. At the same time, the field distributions corresponding to the excited resonances are substantially different depending on the choice of the substrate. Clearly distinguishable radiation cones (shaped as horizontal “V” with varying opening angles) are visible in the effective medium substrate, but they are suppressed in metal-dielectric slab (cf. Fig. 4 in Ref. [30]). This is the result of the near-field interaction of the nanoparticle with the first metal layer, leading to the breakdown of the effective medium approach valid for plane waves. Measuring the values of radiation opening angles at the resonant wavelengths in the far-field after passing through the substrate gives the opportunity to determine the type of a nanoparticle resonance. The magnetic moment of the particle at the magnetic dipole resonance is reduced on the metamaterial substrate in both descriptions, and other moments are slightly increased. The presence of hyperbolic metamaterial reduces the reflection of the incident wave from the substrate. The scattering particle has an access to the high-density of states in the substrate, reducing the backscattering efficiency. This complex interplay results in the aforementioned changes of the values of moments. Interestingly, while the field profiles inside the metamaterial substrate are remarkably different in the layered and homogeneous realizations, the overall system’s responses in the far field above the substrate are similar.

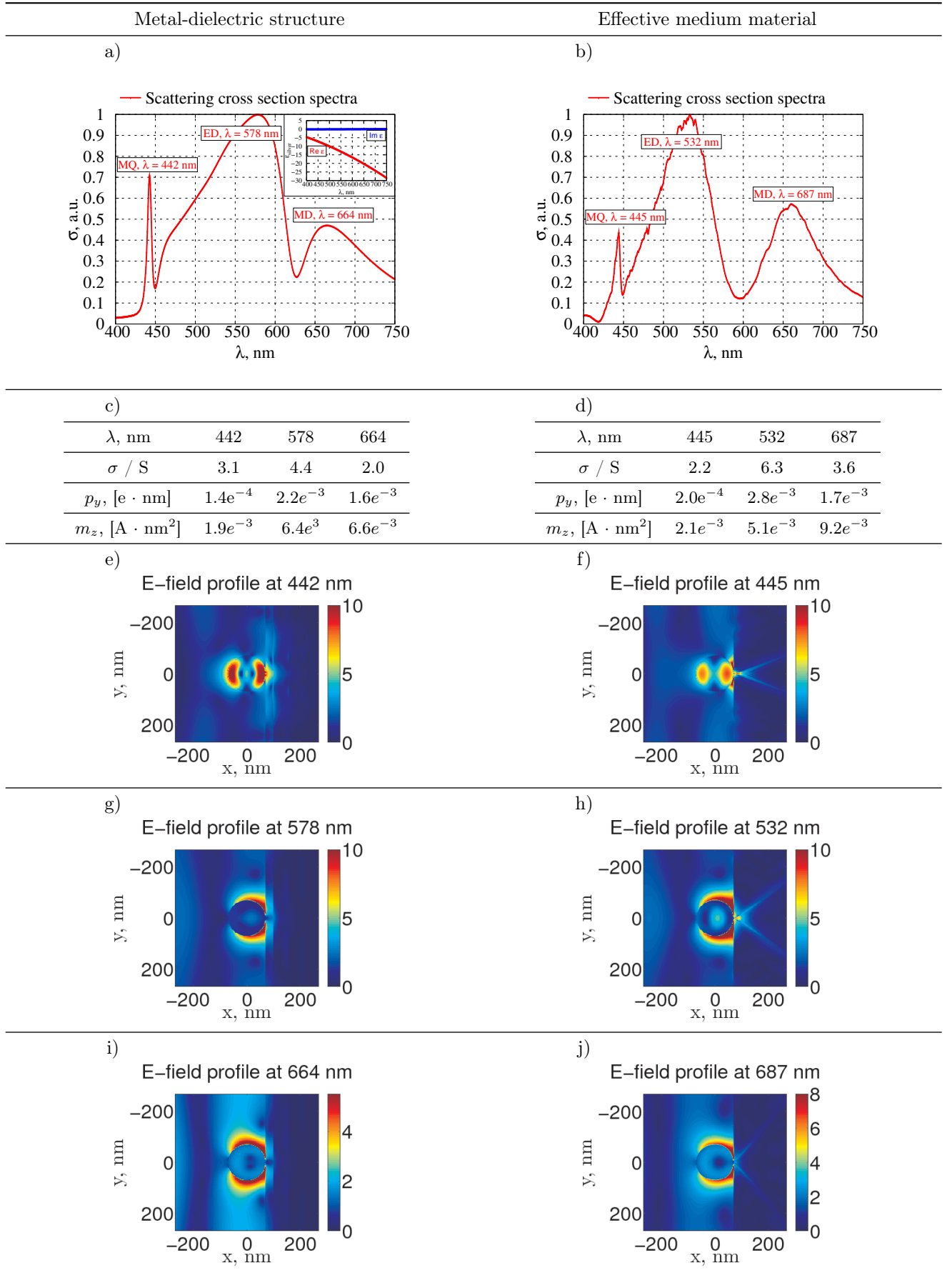


Fig. 7: Optical properties of a dielectric nanoparticle ($\epsilon_{particle} = 20$) of 70 nm radius on (a,c,e,g,i) a metal-dielectric multilayered substrate ($\epsilon_{dielectric} = 3.1$, see the inset in (a) for ϵ_{silver}) and (b,d,f,h,j) an effective homogeneous medium with the effective permittivity as in Fig. 6: (a,b) scattering cross-section spectra, (c,d) the summary of the resonant wavelengths, the scattering cross-section normalised to the geometric cross-section, and electric p_y and magnetic moments m_z , (e-j) the spatial distribution of the electric field amplitudes at resonant wavelengths (normalised to the incident field).

4 Conclusion and outlook

In this paper, we performed comprehensive numerical studies of the substrate influence on the optical properties of high-index dielectric nanoparticles. Different types of substrates such as flint glass, perfect electric conductor, gold, and hyperbolic metamaterial were investigated. Retardation effects were shown to play significant role in the particle-substrate interactions making the “classical” tools such as image theory to be of limited applicability even in the case of a PEC substrate. Moreover, substrates supporting nontrivial electromagnetic excitations such as surface plasmon polaritons in case of plasmonic metals and high-density of states extraordinary waves in the case of hyperbolic metamaterials, give rise to complex resonant responses and open a possibility for on-demand tailoring of optical properties. The presence of substrates was shown to introduce significant impact on particle’s magnetic resonances and resonant scattering cross-sections. As for overall comparison of different substrates, we can observe that dispersionless dielectric substrates are the best for preserving natural properties of individual particles, PEC and metal-dielectric substrates give a relatively strong the MQ resonance and the best enhancement of the ED resonance, and gold substrate is beneficial for the MD resonance. Variation of substrate material provides an additional degree of freedom in tailoring properties of emission of magnetic multipoles and designing Fano-like resonances combining magnetic and electric excitations.

5 Acknowledgements

This work was supported, in part, by the government of the Russian Federation (Grant 074-U01 and 11.G34.31.0020) and EPSRC (UK). AZ acknowledges support from the Royal Society and the Wolfson Foundation. Authors acknowledge discussions with Prof. Yuri S. Kivshar and Dr. Andrey Miroshnichenko.

References

- [1] W. J. Polydoroff, W. Polydoroff (J.), and J. Wiley, “High-frequency Magnetic Materials: Their Characteristics and Principal Applications,” Front Cover , 1960 - Magnetic materials - 220 pages
- [2] D. R. Smith, W. J. Padilla, D. C. Vier, S. C. Nemat-Nasser, and S. Schultz, "Composite Medium with Simultaneously Negative Permeability and Permittivity Phys. Rev. Lett. 84, 4184–4187 (2000).
- [3] N. I. Zheludev, “The road ahead for metamaterials”, Science 328, 582–583 (2010).
- [4] Soukoulis, C. M. and Wegener, M. Optical metamaterials – more bulky and less lossy. Science 330, 1633–1634 (2010).
- [5] Boltasseva, A. and Atwater, H. A. Low-loss plasmonic metamaterials. Science 331, 290–291 (2011).
- [6] V. M. Shalaev, “Optical negative-index metamaterials”, Nature Photon. 1, 41–48 (2007).
- [7] I. P. Radko, S. I. Bozhevolnyi, A. B. Evlyukhin, and A. Boltasseva, "Surface plasmon polariton beam focusing with parabolic nanoparticle chains," Opt. Express 15, 6576-6582 (2007).
- [8] P. Ginzburg, N. Amir, N. Berkovitch, A. Normatov, G. Lerman, A. Yanai, U. Levy, and M. Orenstein, “Plasmonic resonance effects for tandem receiving-transmitting nano-antennas”, Nano Lett. 11, 220–224 (2011).
- [9] A. G. Curto, G. Volpe, T. H. Taminiau, M. P. Kreuzer, R. Quidant, and N. F. van Hulst, “Unidirectional emission of a quantum dot coupled to a nanoantenna”, Science 329, 930-933 (2010).
- [10] A. V. Zayats, I. I. Smolyaninov, A. A. Maradudin, “Nano-optics of surface plasmon polaritons," Phys. Rep. 408, 131 - 314(2005).
- [11] Maier SA, Kik PG, Atwater HA, 2002, Observation of coupled plasmon-polariton modes in Au nanoparticle chain waveguides of different lengths: Estimation of waveguide loss, Applied Physics Letters, Vol:81, ISSN:0003-6951, Pages:1714-1716
- [12] A. B. Evlyukhin, C. Reinhardt, A. Seidel, B. S. Luk'yanchuk, and B. N. Chichkov, “Optical response features of Si-nanoparticle arrays”, Phys. Rev. B. 82, 045404, (2010).
- [13] J. N. Anker, W. P. Hall, O. Lyandres, N. C. Shah, J. Zhao, and R. P. Van Duyne, “Biosensing with plasmonic nanosensors”, Nature Materials 7, 442 - 453 (2008).

- [14] A. E. Krasnok, A. E. Miroschnichenko, P. A. Belov, and Yu. S. Kivshar, "All-dielectric optical nanoantennas," *Opt. Express* 20, 20599-20604 (2012).
- [15] A. B. Evlyukhin, S. M. Novikov, U. Zywietz, R. L. Eriksen, C. Reinhardt, S. I. Bozhevolnyi, and B. N. Chichkov, "Demonstration of Magnetic Dipole Resonances of Dielectric Nanospheres in the Visible Region", *Nano Lett.* 12, 3749-3755 (2012).
- [16] A. I. Kuznetsov, A. E. Miroschnichenko, Y. H. Fu, J. Zhang, and B. Luk'yanchuk, "Magnetic Light", *Nature: scientific reports*, DOI: 10.1038/srep00492, (2012).
- [17] Y. H. Fu, A. I. Kuznetsov, A. E. Miroschnichenko, Y. F. Yu and B. Luk'yanchuk, "Directional visible light scattering by silicon nanoparticles", *Nat. Commun.* 4:1527 doi: 10.1038/ncomms2538, (2013).
- [18] C. F. Bohren and D. R. Huffman, "Absorption and scattering of light by small particles", Wiley-VCH, 1998
- [19] P. Hammond, "Electric and magnetic images", *Proc. IEE*, vol. 107C, 306 -313 (1960).
- [20] J. A. Fan, K. Bao, J. B. Lassiter, J. Bao, N. J. Halas, P. Nordlander, and F. Capasso, "Near-Normal Incidence Dark-Field Microscopy: Applications to Nanoplasmonic Spectroscopy", *Nano Lett.* 12 (6), 2817-2821, (2012).
- [21] N. Berkovitch, P. Ginzburg and M. Orenstein, "Nano-plasmonic antennas in the near infrared regime", *J. Phys.: Condens. Matter* 24, 073202, (2012).
- [22] F. Moreno, J. M. Saiz, and F. González, "Light Scattering by Particles on Substrates. Theory and Experiments", at *Light Scattering and Nanoscale Surface Roughness Nanostructure Science and Technology*, pp 305-340 (2007).
- [23] J. L. de la Pena, F. Gonzales, J. M. Saiz, P. J. Valle, and F. Moreno, "Sizing particles on substrates: a general method for oblique incidence", *J. Appl. Phys.* 85, 432-438 (1999)
- [24] P. A. Bobbert, J. Vlieger, "Light scattering by a sphere on a substrate", *Physica A* 137, 243-257 (1986)
- [25] I. V. Lindell, J. J. Hanninen and K. I. Nikoskinen, "Electrostatic image theory for an anisotropic boundary", *Science, Measurement and Technology, IEE Proceedings -* , vol.151, no.3, pp.188,194, (2004).
- [26] A. E. Krasnok, D. S. Filonov, A. P. Slobozhanyuk, P. A. Belov, C. R. Simovski, and Yu. S. Kivshar, "Superdirective magnetic nanoantennas with effect of light steering: Theory and experiment", *Microwave and Optoelectronics Conference (IMOC)*, pp. 1-3, 2013
- [27] A. Taflov, S. C. Hagness, *Computational Electrodynamics: The Finite- Difference Time-Domain Method*, Artech House, INC., 685 Canton Street Nordwood, MA, 02062
- [28] S. A. Maier, "Plasmonics: Fundamentals and Applications", Springer, DOI:10.1007/0-387-37825-1, 2007
- [29] P. B. Johnson and R. W. Christy, "Optical constants of the noble metals", *Phys. Rev. B* 6, 4370-4379 (1972)
- [30] P. Ginzburg, A. V. Krasavin, A. N. Poddubny, P. A. Belov, Yu. S. Kivshar, and A. V. Zayats, "Self-Induced Torque in Hyperbolic Metamaterials", *Phys. Rev. Lett.* 111, 036804 (2013).
- [31] P. V. Kapitanova, P. Ginzburg, F. J. Rodríguez-Fortuño, D. S. Filonov, P. A. Belov, A. N. Poddubny, Yu. S. Kivshar, G. A. Wurtz, and A. V. Zayats, "Photonic Hall effect in Metamaterials: Polarization-controlled routing of subwavelength electromagnetic modes in hyperbolic metamaterials composites", *Nature Communications* (2014) DOI: 10.1038/ncomms4226.
- [32] A. N. Poddubny, I. Iorsh, P. A. Belov, and Yu. S. Kivshar, "Hyperbolic metamaterials", *Nature Photonics* 7, 948-957, (2013).
- [33] Ya. B. Fainberg, N. A. Khizhnyak, "Artificial anisotropic media", *JETP*, 25, p.711, 1955
- [34] A. A. Orlov, A. V. Chebykin, and P. A. Belov, "Strong spatial dispersion in nanostructured multilayered metal-dielectric optical metamaterials", *Proc. SPIE*, vol. 7754, pp. 77540E(1-7), 2010